2021 43rd Annual International Conference of the
IEEE Engineering in Medicine & Biology Society (EMBC)
Oct 31 - Nov 4, 2021. Virtual Conference

Estimating Pulsatile Blood Flow Parameters from Digital Subtraction Angiography*

Ko-Kung Chen, PhD, Chung-Jung Lin*, MD, Wei-Fa Chu

Abstract— **Digital subtraction angiography (DSA) is the gold standard for diagnosing vascular diseases. Much attention had been attracted on estimating blood flow velocity from DSA data, and many techniques to compute the mean flow velocity had been proposed. In this paper, we present a physical model that demonstrates how the pulsatile flow can affect the dispersion of the contrast medium delivered into the blood vessel. Using empirical mode decomposition and angiographic data of 4 patients, we then showed it is feasible to compute pulsatile flow related parameters from routine interventional angiographic acquisitions.**

Clinical Relevance— **This is the first attempt to present a physical model and corresponding method to estimate pulsatile flow related parameters from routine angiographic acquisitions, and has potential to be used for real-time diagnostic and therapeutic monitoring during interventional procedures.**

I. Introduction

Digital subtraction angiography (DSA) is considered as criterion standard for imaging vascular diseases. While DSA resolves contrast medium in a blood vessel with good spatial and temporal resolution, its inherent hemodynamic characteristics has not been investigated in detail, and remains largely unused clinically. As literature had suggested good relationships between hemodynamics and various vascular diseases, such as atherosclerosis, aneurysm formation, and arteriovenous malformation [1,2], a real-time hemodynamic measurement using DSA potentially facilitate peritherapeutic monitoring and treatment decision. However, experimental measurement in individual flows remains challenging, as diverse vascular geometry leads to complex flow patterns.

Within the context of interventional imaging, blood flow measurements had often been carried out using 2D DSA [3,4], or a combination of 2D DSA and 3D vascular anatomy derived from other imaging modalities [5-8]. Methods for deriving blood flow velocities can be divided into contrast bolus tracking and computational approaches. Despite the blood flow is pulsatile per se, these proposed techniques yield mean velocities only. More recently, we presented a physical model to show that the motion of mixture of contrast medium and blood obeys a 1-D advection equation in a tubular blood vessel, and develop an algorithm that has potential to estimate the pulsatile velocity [9].

In this paper, we use basic periodically varying pulsatile flow in our model, and calculate the characteristic contrast medium pattern induced by pulsatile flow. From the numerical simulations of the model prediction, we found the time evolutions of the contrast waves often exhibited non-symmetric sinusoidal pattern, and similar structure can also be observed in our collected real angiographic data. While similar patterns had previously been shown in Bonnefous and his colleagues' work (Figure 2 in [7]), the subtle pattern of pulsatile induced contrast medium distribution had not attracted the authors' attention.

Using Huang's empirical mode decomposition method [10], we then showed that it is feasible to derive pulsatile velocity of tubular blood vessels from routine angiographic acquisitions. Huang's method had been shown to be effective of analyzing signals of non-stationary and changing frequency. This method decomposes the original time signal into separate modes with different frequencies. Each mode has zero mean, and the corresponding phase can be computed using Hilbert transform.

By retrospectively analyzing 4 patients who underwent angiographic examinations, we found that the contrast medium, being advected by the fast and slow components of pulsatile blood flow, can exhibit frequency modulations in a single cycle, we then calculate the corresponding phases change and identify the fast and slow components of the blood flow, and compute the velocity ratio of fast flow to the slow flow.

II. Methods

A. Physical model

Chen et al concluded that in a tubular vessel, the delivered contrast medium, advected by the blood flow, obeys an 1-D advection equation [9], i.e.,

$$\frac{\partial C}{\partial t} + w\frac{\partial C}{\partial z} = 0 \ldots \text{eq}(1)$$

where w, t, z, and C are the blood flow velocity, time, axial distance, and angiographic signal, respectively.

Consider $\eta = z - \int_0^t w(t')dt'$, one may show that C is a function of η only. Choose $C = \cos(k\eta)$, i.e.,

$$C(z,t) = \cos k\left(z - \int_0^t w(t')dt'\right) \ldots \text{eq}(2)$$

where k is the wave number in the axial direction.

Let w take the form of a periodically varying sinusoidal function plus a mean value,

*Research supported in part by 109-2628-B-010-014, Ministry of Science, Taiwan, R.O.C., and in part by Siemens Healthcare.

Ko-Kung Chen is with the Department of Medicine, National Yang Ming Chiao Tung University, Taipei, Taiwan, R.O.C. (e-mail: kkchen0438@gmail.com).

*Chung-Jung Lin is with both the Department of Medicine, National Yang Ming Chiao Tung University, Taipei, Taiwan, R.O.C., and Taipei Veteran General Hospital, Taipei, Taiwan, R.O.C. (corresponding author to provide phone: +886 2 2871 2121 #3041; e-mail: bcjlin@gmail.com).

Wei-Fa Chu is with Taipei Veteran General Hospital, Taipei, Taiwan, R.O.C. (e-mail: wfchu2320@gmail.com).

$$w = w_0 + w_p \cos(\Omega t) \ldots eq(3)$$

where Ω is the frequency of the sinusoidal function. Substitute it into eq(2) yields

$$C(z,t) = \cos\varphi = \cos\left(kz - kw_0 t - \frac{kw_p}{\Omega}\sin\Omega t\right) \ldots eq(4)$$

where φ is the phase function. The eq(4) shows how the pulsatile velocity w modulates the dispersion of the contrast medium C.

At any fixed position z, the local frequency is defined as the derivative of φ with respect to t, i.e.,

$$\frac{\partial\varphi}{\partial t} = -kw_0 - kw_p\cos\Omega t = -kw \ldots eq(5)$$

which implies that for the pulsatile blood flow with constant longitudinal wave number, the change in blood flow velocity is directly proportional to the local frequency, hence the velocity ratio of the fast to the slow flow may be estimated regardless of the wave number.

B. *Qualitative comparison of numerical experiment and angiographic signals*

In the following numerical simulations, we set w_0 and w_p as 10-cm/s, and the frequency is 1-Hz, as shown in figure 1.

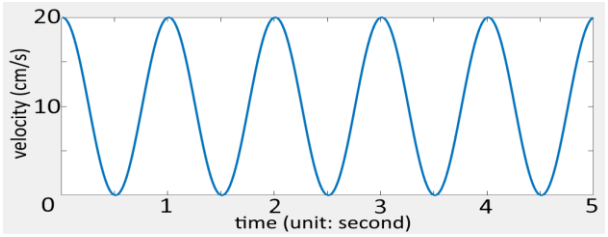

Figure 1. A 1-Hz sinusoidal velocity function that varies from 0-cm/s to 20-cm/s.

Using this artificial velocity function, the modulated contrast medium pattern generated from eq(4) is shown in figure 2. Five signals at different axial position, with an interspacing of 80-mm between consecutive signals, are plotted at the right. In addition to periodically nature of the contrast waves along the time, the contrast wave also exhibits non-symmetrical pattern. Within a single cycle along the time, the form of non-symmetric contrast wave also evolves slightly as it travels downstream.

Similar phenomenon can be seen in Figure 2 of Bonnefous' work [7]; our angiographic signals also show similar patterns (Figure 3). The qualitative similarity of Bonnefous' angiographic observations, our own real angiographic data, and our model predictions suggests that eq(4) may well demonstrate how pulsatile flow modulates the dispersion of the contrast medium delivered into a tubular blood vessel.

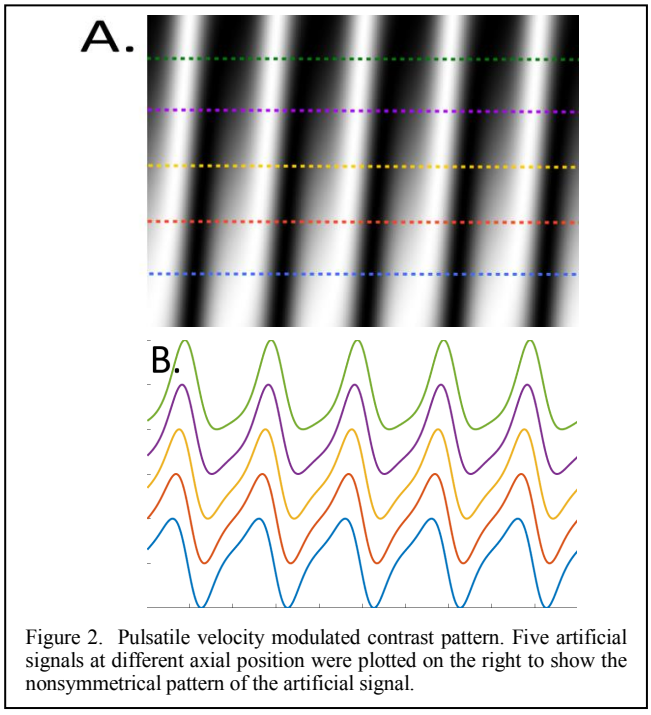

Figure 2. Pulsatile velocity modulated contrast pattern. Five artificial signals at different axial position were plotted on the right to show the nonsymmetrical pattern of the artificial signal.

C. *Estimate pulsatile velocity related parameters*

Theoretically, a complete pulsatile velocity function can be constructed by evaluating the instantaneous frequency of all angiographic signals; in practice, however, blood vessel segments with sufficient axial length to resolve wave number along axial direction are usually unavailable, and presence of

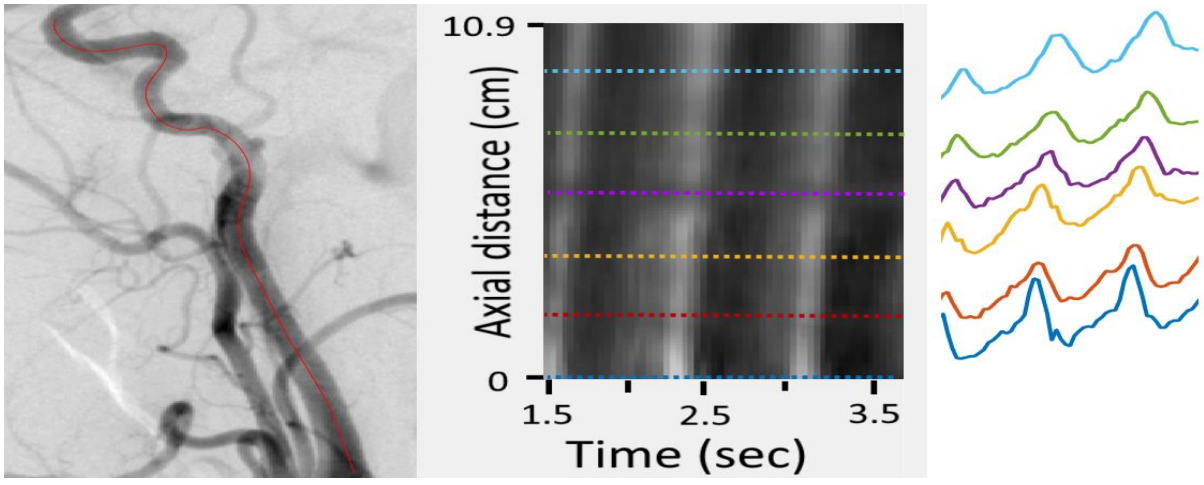

Figure 3. A 10.9-cm long vascular centerline (red line) is first estimated from 3D rotational angiography and registered onto corresponding 2D-DSA images. The Angiographic signals, from 1.5-s to 3.5-s, along the center line are plotted. 6 angiographic signals, that are sampled along the center line with an interspacing of 2-cm, also show non-symmetrical characteristics.

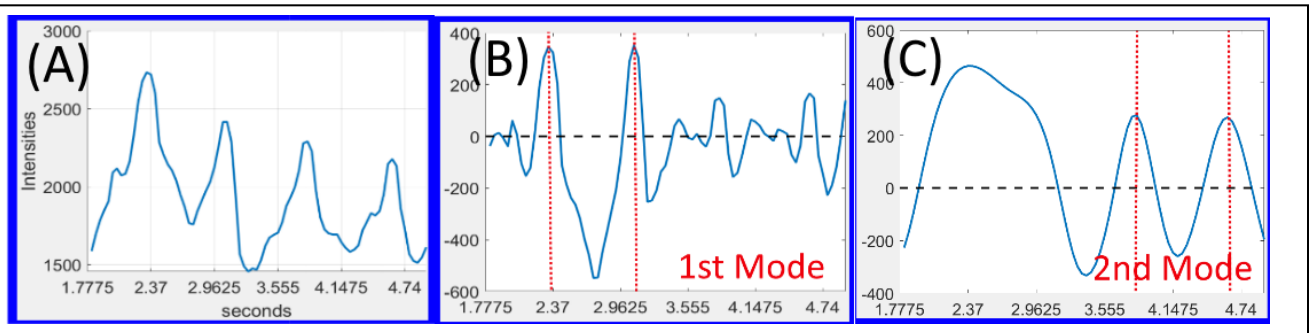

Figure 4. (A) A segment of typical angiographic signal. (B) The first empirical mode of Huang's empirical mode decomposition. Dotted red lines mark the time span used for computing the phases using Hilbert transform. (C) The second empirical mode.

artefacts and noise also make analytic approaches for pulsatile velocity difficult.

Since the angiographic signals, modulated by a pulsatile basic flow, appears to be non-stationary and frequency-changing, one may adopt the Hilbert Huang Transform to analyze them, and form the corresponding empirical modes decompositions. Each empirical mode, except the hump, may consist of realizations with different periods, but there is just one wave at any time instant and with zero local mean.

Figure 4A shows a segment of typical angiographic signal that exhibits periodically varying contrast waves. The period of these waves is closely related to cardiac cycle. In the first mode (Figure 4B), the time of the peak positions associated with the first two pulses tallies with that of the original contrast waveforms; however, there exist higher frequency signal in the rest period of this mode. This higher frequency component has much lower intensity and is not directly associated with the cardiac cycle. In the second mode (Figure 4C), there are three pulses during the steady time span, the first one has a period much longer than the rest two pulses, and this variation has no link to the cardiac cycle. Hence, the first two waves in mode one and the last two waves in mode two were choose to study the phase variation of the contrast medium in a single contrast wave. Hilbert transform were performed on these two signal segments from the peak to peak time interval, as indicated by the red lines in Figure 4B and Figure 4C.

The computed phases are shown in polar plots in Figure 5. In polar plot, the space between adjacent lines represent advancing phase in a single time frame. At certain time frames, it is visible that some gaps between adjacent lines are wider, which corresponds to higher angular velocity, hence flow velocity, as implied by eq(5). Binomial classification method was used to classify the phase change rates into two groups. The red lines and blue lines in the polar plots are time steps classified as fast and slow flow components. Based on the binomially classified results, the phase change rates for each category were averaged:

$$\text{Pfast} = \frac{1}{n}\sum_{b=1}^{b=n} \text{Pf}_b,\ \text{Pslow} = \frac{1}{m}\sum_{a=1}^{a=m} \text{Ps}_a$$

where Pf and Ps are the phase change rates classified as fast flow and slow flow components, respectively. The blood flow velocity ratio Vr is then defined as the average phase change rate of fast flow fraction over that of the slow flow fraction:

$$\text{Vr} = \frac{\text{Pfast}}{\text{Pslow}}$$

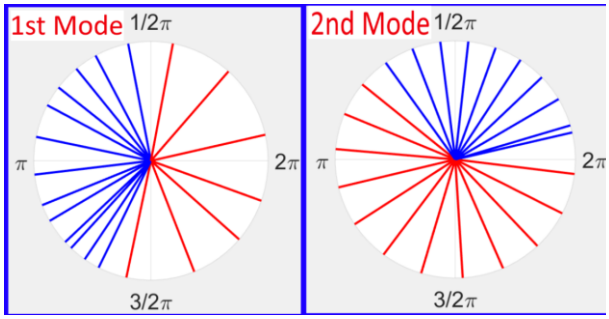

Figure 5. The polar plots of the computed phases of the first and second modes. The red and blue lines denote the time frames that are classified as fast and slow flow component in one contrast wave, respectively.

III. Results and Discussion

We set up numerical experiments using different velocity profiles, and estimate the velocity ratio using proposed method. For each numeric test, the reference velocity ratio was obtained by taking the zero amplitude as baseline to divide velocity profile into fast and slow moving periods first (Figure 6), followed by averaging velocities during each period. The velocity ratio of fast to slow period was computed by dividing the mean velocity during fast period with mean velocity during slow period. The parameters and estimated ratio were given in Table 1.

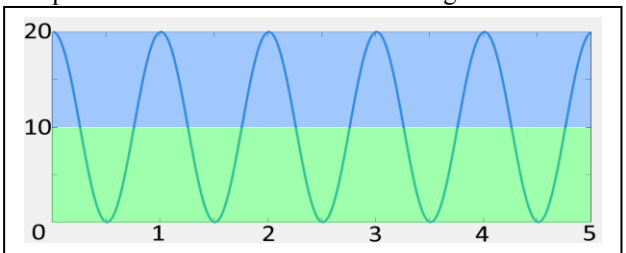

Figure 6. Using zero amplitude as base line, the generated velocity profile is divided into faster (blue) and slower (green) period. Mean velocity during fast and slow periods were computed.

TABLE I. *Parameters and Estimated Velocity Ratio in Numeric Experiments.*

Numeric test number	*Mean W_0 (cm/s)*	*Amplitude W_p (cm/s)*	*Estimated velocity ratio*	*Reference velocity ratio*
1	10	10	1.89	4.3
2	4.95	3.3	1.53	2.42

Numeric test number	*Mean W_0 (cm/s)*	*Amplitude W_p (cm/s)*	*Estimated velocity ratio*	*Reference velocity ratio*
3	5	2.5	1.39	1.90
4	4.95	1.65	1.24	1.52
5	8.1	4.5	1.30	2.06
6	6	5	1.64	3.16
7	5.2	4	1.64	2.84
8	5.6	4	1.56	2.60
9	7.5	5	1.46	2.42
10	7.2	6	1.60	3.16

It is important to note that, despite the trend of estimated ratio tallies with that of reference velocity ratio (r=0.96), there exist differences between the two velocity ratios. Such discrepancy may be attributed to the binomial classification adopted, and the frequency modulation during Hilbert Huang Transform. How these factors influence the estimated velocity ratios warrant further investigations.

Additionally, after receiving the institutional review board approval, we retrospectively analyzed 4 patients who underwent DSA examinations. The mean flow velocity is computed using Chen's method [9], and velocity ratio is computed using proposed technique. The results are summarized in Table 2.

TABLE II. *THE ESTIMATED PARAMETERS PLUS ONE STANDARD DEVIATION OF RECRUITED PATIENTS.*

Patient number	*Mean blood flow velocity (cm/sec)*	*Mean velocity ratio of $\frac{fast\ flow}{slow\ flow}$*
1	23.06	1.51±0.15
2	23.59	1.83±0.10
3	37.44	1.82±0.22
4	38.28	2.02±0.41

In comparison to Doppler ultrasound, the commonly reported peak systolic flow velocities of relatively normal internal carotid artery fall around 100-cm/second, though individual value can vary greatly; The reported end diastolic velocities fall around 40-cm/second [11,12]. Dividing the reported peaks systolic velocity by the end diastolic velocity gives a ratio about 2.5. Our estimated velocity ratios are lower than the average reported value. It should be noted, however, both the numerator and the denominator of our estimated velocity ratio are the averaged velocities over a certain time span, while the peaks systolic velocity and end diastolic velocity are the fastest and slowest velocities within a cardiac cycle, hence the estimated velocity ratios using averaged velocities would be theoretically lower.

Another limitation of the current study lies in tiny population, which comprise only 4 patients, whose estimated velocity ratios have no other clinical measurements to compare to. The present study focus on feasibility to derive parameters related to pulsatile blood flow, that can be theoretically justified by physics associated with mixture of contrast medium and blood, from X-ray angiographic images. The detailed interaction between the pulsatile blood flow and the dispersion of contrast medium, as well as how the exact pulsatile blood flow velocity can be estimated from angiographic images remain to be explored. A larger patient population is also warranted in the subsequent study.

IV. CONCLUSION

The pulsatile blood flow modulates the dispersion of contrast medium delivered into blood vessel, resulting in non-symmetrical contrast waves. We proposed a physical model that can be used to study the dispersion of contrast medium released into blood vessel, and show it is feasible to compute pulsatile velocity ratio by evaluating the instantaneous frequency of the angiographic signals.

REFERENCES

[1] Brands P J, Hoeks A P, Hofstra L and Reneman R S 1995 A noninvasive method to estimate wall shear rate using ultrasound Ultrasound Med. Biol. 21 171–85.

[2] Reneman R S and Hoeks A PG2008 Wall shear stress as measured in vivo: consequences for the design of the arterial system Med. Biol. Eng. Comput. 46 499–507.

[3] Huang, T.C., Chang, C.K., Liao, C.H., Ho, Y.J.: Quantification of blood flow in internal cerebral artery by optical flow method on digital subtraction angiography in comparison with time-of-flight magnetic resonance angiography. PLoS One (2013).

[4] Koirala, N., McLennan, G.: Blood flow quantification in dialysis access using digital subtraction angiography: a retrospective study. Comput. Methods Programs Biomed. 190, 105379 (2020).

[5] Waechter, I., Bredno, J., Hermans, R., Weese, J., Barratt, D.C., Hawkes. D.J.. Model-based blood flow quantification from rotational angiography. Med Image Anal. 2008 Oct;12(5):586-602. doi: 10.1016/j.media.2008.06.003. Epub 2008 Jun 18.

[6] Shaughnessy G, Schafer S, Speidel MA, Strother CM, Mistretta CA. Measuring blood velocity using 4D-DSA: A feasibility study. Med Phys. 2018 Oct;45(10):4510-4518. doi: 10.1002/mp.13120.

[7] Bonnefous O, Pereira VM, Ouared R, Brina O, Aerts H, Hermans R, van Nijnatten F, Stawiaski J, Ruijters D. Quantification of arterial flow using digital subtraction angiography. Med Phys. 2012 Oct;39(10):6264-75. doi: 10.1118/1.4754299.

[8] Andrew D Copeland, Rami S Mangoubi, Mukund N Desai, Sanjoy K Mitter, Adel M Malek. Spatio-Temporal Data Fusion for 3D+T Image Reconstruction in Cerebral Angiography. IEEE Trans Med Imaging. 2010 Jun;29(6):1238-51. doi: 10.1109/TMI.2009.2039645.

[9] Ko-Kung Chen, Chung-Jung Lin, Wan-Yuo Guo, Wei-Fa Chu, Yu-Te Wu. Estimating blood flow velocity using time-resolved 3D angiography and a derived physical law of contrast media. 2021 Physiol. Meas. 42 025007

[10] Norden E. Huang, Zheng Shen, Steven R. Long, Manli C. Wu, Hsing H. Shih, Quanan Zheng, Nai-Chyuan Yen, Chi Chao Tung, Henry H. Liu The Empirical Mode Decomposition and the Hilbert Spectrum for Nonlinear and Non-Stationary Time Series Analysis. Proceedings of the Royal Society of London. 1998. Series A, Vol. 454, pp. 903-995

[11] Bouthier J, Benetos A, Simon A, et al. Pulsed Doppler: An Evaluation of Diameter, Blood Velocity and Blood. J Cardiovasc Pharmacol. 1985;7 Suppl 2:S99-04.

[12] Kochanowicz J, Mariak Z, Rutkowski R, et al. Age and sex dependency of blood flow velocity in the internal carotid. Neurol Neurochir Pol. 2009 Jan-Feb;43(1):3-8.